Kinetics and Functional Parameters Response of Aluminum Sulphate Coagulant to Variation in Coag-Flocculation Variables in High Turbid Pharmaceutical Industry Effluent

Ugonabo, V. I, Menkiti, M .C, Onukwuli, D. O, Igbokwe, P.K

Abstract:- The kinetic and functional parameters behavior of alum in respect of pH dosage and time variation in high turbid pharmaceutical industry effluent has been investigated at room temperature. Kinetic and functional parameters such as order of reaction α, rate constants (K and K_R), coagulation period $\tau_{1/2}$ etc were determined. Turbidity measurement was carried out using model 212R Turbid meter. The maximium alum performance are recorded at K of $1.34 \times 10^{-4} m^3/kg.s$, dosage of $0.1 \times 10^{-3} m^3/$, pH of 10 and $\tau_{1/2}$ of 8.11 sec. the maximum value of E(%) recorded after 40 minutes (2400 sec) is 93.26%, thus confirming alum as effective coag-flocculant. In general, the value obtained indicates that the theory of micro kinetics holds for coagulation – flocculation of pharmaceutical industry effluent using alum at the conditions of the experiment.

Keywords: **Alum, Coag-flocculation variables, kinetics, pharmaceutical effluent.**

I. INTRODUCTION

The persistent presence of pharmaceuticals in a natural environment has always pose potential risk to both man and animals alike and it can disturb the ecological balance. Pharmaceutical industry effluent (PIE) is mainly generated via the washing activities of the equipment after batch operations. Though the effluent discharged is small in volume, but highly polluted due to the presence of reasonable amount of organic pollutants [1],[2]. The level of the effluent pollution varies, depending on the product manufactured, the materials used in the process, and other process details [3],[4]. PIE, generated from the equipment washing activities after each batch operations contains large amount of Chemical Oxygen Demand (COD), Turbidity total dissolve solid particles (TDSP), Biological oxygen demand (BOD) and colloidal particles creating pollution problem, if discharged untreated [5],[6]. It has been reported that PIE on average has BOD (1450mg/l); COD (2500mg/l); total alkalinity; (75mgl CaCO$_3$), total suspended solid (350mg/l); PH (6.8), and phenol (68.5mg/l) [7],[8]. Owing to the fact that reasonable quantity of the solids in the effluent posses colloidal characteristics, it cannot be removed by mere gravitational settling. Thus a need for appropriate treatment option becomes imperatives. Coagulation/ flocculation techniques can be applied to these ends bearing in minds its inherent qualities such as being cheap, potable and requires low operator skill.

Coagulation/flocculation process is employed in water and waster water treatment. It involves addition of coagulant (aggregating agents) to facilitate destabilization of the suspended particle's charges which result in particles agglomeration into larger settle able flocs [9],[10]. This process also plays important role in surface water treatment by reducing turbidity, colour, bacteria, algae, organic matter and clay particles [9],[11],[12]. Early bench, pilot and demonstration scale studies have shown that pollutants in industrial/ domestic effluents can be efficiently removed during coagulation with alum and ferric chloride even when present at low or high concentrations [13] . Traditional aluminum (Al) based salt (AlCl$_3$ and alum) are most commonly used in water treatment plants. On addition to effluent Al coagulant dissociates and Al$_3^+$ ions undergo hydrolysis reaction to form Al species which are usually divided into monomeric species(e.g.Al_3^+,$Al(OH)_2^+$,$Al_2(OH)_2^{4+}$,$Al_3(OH)_4^{5+}$,medium polymer species (e.g.,$AlO_4Al_{12}(OH)_{24}(H2O)_{12}^{7+}$,$Al_{13}$), colloidal or precipitate or solid species [13],[14],[15],[16],[17]. The degree to which the reactions are proceeded and the nature of the produced species may depend on coag-flocculation variables such as coagulant dosage, pH, time, temperature and the presence of any other ions. Al species during coagulation process play a key role in determining the behavior and efficiency of Al based coagulants. Thus previous researchers paid more attention to the effect of Al speciation on coagulation performance with little or nothing to coag-flocculation kinetics which arouses the authors interest in this work. During coag-flocculation process, the suspended and total dissolved particles in the effluents are generally, removed via two main mechanisms including precipitation of large volume of hydroxide flocs and adsorption on formed flocs [17]. However, amongst the aluminum (Al) based salt coagulants, alum (aluminum suphate) have been reported to be better because it is easy to handle and apply and most importantly produces less sludge. It's primary disadvantage is that it is most effective over a limited pH range of 6.5 – 7.5 [18]. The purpose of this work is to study the coagulation – flocculation kinetics of alum (aluminum sulphate) in PIE, in the removal of both total suspended and dissolved particles during coagulation

flocculation process. In addition to determining the effect of the variation in the coagulation – flocculation variables (dosage, settling time, pH etc) in the removal of both total suspended and dissolved particles was conducted.

II. THEORETICAL PRINCIPLES AND MODEL DEVELOPMENT

For a homogenous micro kinetic particles in equilibrium state with minimal influence of attractive and repulsive forces respectively [19],[20],[21].

$$\mu_i = U_i = \left(\quad \right) nS, nV, n_j \qquad (1)$$

Also

$$\mu_i = G_i = \left(\quad \right) p, T, n_j = \text{a constant} \qquad (2)$$

Thus $\mu_i = G_i = 0$ $\qquad (3)$

$$D^1 = \frac{K_B T}{B} \qquad (4)$$

Where D^1 is diffusion coefficient
  B is friction factor
  K_B is Boltzman constant (molar gas constant) per particle The general model for micro kinetic coagulation – flocculation of mono dispersed particles under the influence of Brownian motion is given as[22].

$$\frac{dC_k}{dt} = \tfrac{1}{2} \sum_{i+j=k} \alpha \beta_{BR} (V_i, V_j) C_i C_j - \sum \alpha \beta_{BR}(V_i,V_j)C_i C_k \qquad (5)$$

Where $\frac{dC_k}{dt}$ is the rate of depletion of concentration of particle size K (Conc/ time)

α is the fraction of collisions that result in particle attachment.

β_{BR} is a function of coagulation – flocculation transport for Brownian mechanism.

C_i is the concentration for particle size i

C_j is the concentration for particle size j.

$V_i V_j$ are interaction potentials for particle sizes $_i$ and $_j$ respectively.

The value of B_{BR} for transport mechanism is given as[22].

$$\beta_{BR} = \frac{8}{3} \varepsilon_p \frac{K_B T}{\eta} \qquad (6)$$

Where ε_p is collision efficiency
    η is the viscosity of effluent medium

The general equation representing aggregation rate of particles is obtained by solving the combination of equation (5) and (6) to yield.

$$\frac{dC_t}{dt} = KC_t^{\alpha} \qquad (7a)$$

or

$$dC_t^{\alpha} / C_t = -K \, dt \qquad (7b)$$

Where: C_t is total particle concentration at time t,

$C_t = \Sigma C_K$ (moles/Volume)

K is the αth order of coagulation - flocculation constant.

α is the order of coagulation – flocculation.

And $K = \tfrac{1}{2} \beta_{BR}$ $\qquad (8)$

Also $\beta_{BR} = 2 \Sigma_P K_R$ $\qquad (9)$

Combining equations (7a), (8) and (9) yields

$$- \frac{dC_t}{dt} = \Sigma_P K_R C_t^{\alpha} \qquad (10)$$

Where K_R is the Von smoluchowski rate Constant for rapid coagulation [23]

But $K_R = 8\pi R D^1$ $\qquad (11)$

$R_P = 2a$ $\qquad (12)$

Where a is particle radius

Recall, from Einsteins equation $D1 = \frac{K_B T}{B}$

Where B is the friction factor

$B = 6\pi \eta a$ $\qquad (13)$

Where η is viscosity of coagulating and flocculating medium.

Combining equations (10) to (13) give

$$- \frac{dC_t}{dt} = \frac{4}{3} \Sigma_P \frac{K_B T}{\eta} C_t^{\alpha} \qquad (14)$$

Comparing equations (7a) and (14) show

That $K = \frac{4}{3} \Sigma_P \frac{K_B T}{\eta}$ $\qquad (15)$

For microkinetic aggregation, α theoretically equals 2 [20], [21]

From Fick's Law

$$J_f = D^1 4\pi R_p^2 \frac{dC_t}{dR} \qquad (16)$$

Where: J_f is flux-number of particles per unit surface entering a sphere with radius.

Re-arranging and integrating equation (16) at initial conditions $C_t = 0$, $Rp = 2a$

$$\frac{J_f \int_0^{Rp} \frac{dRp}{R_p^2}}{4\pi D^1} = \int_{Co}^{C_t} dC_t \qquad (17)$$

Therefore, $J_f = 8\pi D^1 a Co$ $\qquad (18)$

In general, for particle of same size under the influence of Brownian motion, the initial rate of rapid coagulation flocculation is

$$- \frac{dc_t}{dt} = Jf.\Sigma p.Co \qquad (19)$$

On substitution of equations (4),(13) and (17) into (19) yield:

$$- \frac{dc_t}{dt} = 8\pi a \frac{K_B T. Co^2 \Sigma_P}{6\pi \eta a} \qquad (20)$$

Thus $- \frac{dc_t}{dt} = \frac{4}{3} \Sigma_P \frac{K_B T. Co^2}{\eta}$ $\qquad (21)$

Similarly at $t > o$

$$- \frac{dc_t}{dt} = \frac{4}{3} \Sigma_P \frac{K_B T. Ct^2}{\eta} \qquad (22)$$

Hence equation (22) has confirmed $\alpha = 2$

For $\alpha = 2$, equation (7) becomes:

$$\frac{dC_t}{dt} = - KC_t^2 \qquad (23)$$

Re-arranging and integrating equation (23) within limits $(0, C_o)$ and $t, C_t)$ give

$$\int_{C_0}^{C_t} \frac{dC_t}{C_t^2} = -K \int_0^t dt \qquad (24)$$

$$\left[\frac{-1}{C_t} \right]_{C_0}^{C_t} = -Kt \qquad (25)$$

Thus

$$\frac{1}{C_t} = Kt + \frac{1}{C_o} \qquad (26)$$

Plot of $(1/C_t)$ vs t produces a slope of K and intercept of $1/C_o$.

From equation (26) making C_t the subject matter yield a relation for the evaluation of coagulation period $(\tau_{1/2})$

$$C_t = \frac{C_o}{1+C_oKt} \qquad (27)$$

Similarly $C_t = \dfrac{C_o}{1 + \dfrac{t}{C_oK}}$ (28)

Putting $\tau_{1/2} = \dfrac{1}{C_oK}$ (29)

Substituting equation (29) into (28), produce

$$C_t = \frac{C_o}{1 + \left[\dfrac{t}{\tau}\right]} \qquad (30)$$

Assume $t = \tau$, then equation (30) yield

$$C_t = \frac{C_o}{2} \qquad (31)$$

Therefore as $C_o \longrightarrow 0.5\, C_o$; $\tau \longrightarrow \tau_{1/2}$

Hence, $\tau_{1/2} = \dfrac{1}{(0.5\, Cok)}$ (32)

For micro kinetic particle aggregation of singlets, doublets and triplets under the influence of Brownian transport mechanism as a function of time $(t \leq 40\ \text{mins})$ at early stages can be obtained by solving equation (7) exactly, resulting in general expression of nth order.

$$\frac{Cn(t)}{Co} = \frac{\dfrac{t}{2}\left[\dfrac{1}{CoK}\right]^{n-1}}{\left[1 + 2\left[\dfrac{1}{CoK}\right]\right]^{n+1}} \qquad (33)$$

Similarly

$$\frac{C_n(t)}{Co} = \frac{\left[\dfrac{t}{\tau^1}\right]^{n-1}}{\left[1 + \dfrac{t}{\tau^1}\right]} \qquad (34)$$

Where $\tau^1 = 2\tau$
And $\tau = \tau_{1/2}$ (35)

Hence for singlets $(n = 1)$

$$C_1(t) = C_o \left[\frac{1}{\left(1 + \dfrac{t}{\tau^1}\right)^2} \right] \qquad (36)$$

For doublets $(n = 2)$

$$C_2(t) = C_o \left[\frac{(t/\tau^1)}{\left(1 + \dfrac{t}{\tau^1}\right)^3} \right] \qquad (37)$$

For triplets $(n = 3)$

$$C_3(t) = C_o \left[\frac{(t/\tau^1)^2}{(1 + t/\tau^1)^4} \right] \qquad (38)$$

Generally equations (36), (37) and (38) represents time evolution of particle size cluster distribution.
Efficiency of coagulation – flocculation is expressed as

$$E\,(\%) = \left[\frac{C_o - C_t}{C_o} \right] 100 \qquad (39)$$

III. MATERIALS AND METHODS

The sample of aluminum sulphate (analytical grade) which has been homogenized to fine powder was sourced from bridge head market located in Onitsha, Anambra state. The pharmaceutical industry effluent sample was collected from a pharmaceutical industry located in Anambra State and characterized as per standard procedure [24], presented in table 1. The Jar test experiment was conducted based on standard Bench scale nephelometric method. Appropriate dose of alum in the range of $(0.1 – 0.7) \times 10^{-3}$ kg/m³ was added to 250ml of the effluent. The suspension, tuned to pH range $1 – 13$ by addition of 10MHCL/ NaOH was subjected to 2 minutes of rapid mixing using 688644A Gulenhamp magnetic stirrer, followed by 40 minutes of settling. During settling, samples were withdrawn from 2cm depth and changes in TSDP measured for kinetic analysis using Lab-Tech model 212R Turbid meter at various time intervals of $2 – 40$ minutes. The whole experiment was carried out at, room temperature. The data obtained were subsequently fitted in appropriate kinetic models for evaluation of coag-flocculation kinetics and functional parameters.

Table 1: Characteristics of Pharmaceutical Industry Effluent Sample before treatment

Parameter	Values
Temperature (^{O}C)	27
Electrical Conductivity (µS/ cm)	4.9
pH	3.87
Phenol (mg/l)	Nil
Odour	acidic
Total hardness (mg/l)	6,000
Calcium (mg/l)	594
Magnesium (mg/l) 250	
Chlorides (mg/l)	100
Dissolved oxygen (mg/l)	20
Biochemical oxygen Demand (mg/l) 5	
Chemical oxygen Demand (mg/l)	1.00
Turbidity (mg/l)	2560
Iron (mg/l)	Nil
Nitrate (mg/l)	Nil
Total acidity (mg/l) 250	
Total viable count (cfu/ml)	9×10^1
Total coli form MPN/ 100 ml	Nil
Total coli form count (cfu/ml)	1×10^1

Faecal count MPN/ ML   Nil

Clostridium perfrigens MPN/ml   Nil

Table 2: Coag-flocculation kinetic parameters and linear regression coefficient of ALUM in PIE at varying pH and $0.1 \times 10^{-3} kg/m^3$ dosage.

Parameters	pH = 1	pH = 3	pH = 5	pH = 7	pH = 10	pH = 13
α	2.000	2.000	2.000	2.000	2.000	2.000
R^2	0.511	0.835	0.849	0.714	0.646	0.906
$K(m^3/kg.S)$	4.0E-06	7.0E-06	7.0E-06	1.0E-05	1.34E-05	1. 2E-05
$K_R(m^3/S)$	1.5366E-19	1.5453E-19	1.5872E-19	1.5571E-19	1.5647E-19	1.5673E-19
$\beta_{BR}(m^3/kg.S)$	8.0E-06	1.4-05	1.4E-05	2.0E-04	2.68E-04	2.4E-05
$\varepsilon_p (Kg^{-1})$	5.2063 E+13	9. 0597E+13	8.8821E+13	1.2844E+15	1.7128E+14	1.53130E+14
$\tau_{1/2}(Sec)$	543.48	207.04	207.04	96.02	8.11	362.32
(-r)	$4.0E-06C_t^2$	$7.0E-06C_t^2$	$7.0E-06C_t^2$	$1.0E-05C_t^2$	$1.34E-04C_t^2$	$1.2E-05C_t^2$
$C_o(kg/m^3)$	707.2136	794.9126	645.9948	548.5464	271.0762	637.3486

Table 3: Coag-flocculation kinetic parameters and linear regression coefficient of ALUM in PIE at varying pH and $0.2 \times 10^{-3} kg/m^3$ dosage.

Parameters	pH = 1	pH = 3	pH = 5	pH = 7	pH = 10	pH = 13
α	2.000	2.000	2.000	2.000	2.000	2.000
R^2	0.837	0.807	0.905	0.673	0.649	0.888
$K(m^3/kg.S)$	2.98E-06	7.08E-06	2.76E-06	2.29E-05	2.35E-05	1. 27E-05
$K_R(m^3/S)$	1.5366E-19	1.5453E-19	1.5872E-19	1.5571E-19	1.5647E-19	1.5673E-19
$\beta_{BR}(m^3/kg.S)$	5.96E-06	1.416-05	5.52E-05	4.58E-05	4.7E-05	2.54E-05
$\varepsilon_p (kg^{-1})$	3.8787 E+13	9. 1633E+13	3.4778E+14	2.9414E+14	3.0038E+14	1.6206E+14
$\tau_{1/2}(Sec)$	929.50	204.70	525.10	42.19	46.25	342.35
(-r)	$2.98E-06C_t^2$	$7.08E-06C_t^2$	$2.76E-06C_t^2$	$2.29E-05C_t^2$	$2.35E-05C_t^2$	$1.27E-05C_t^2$
$C_o(kg/m^3)$	671.5917	766.8712	526.5929 607.1645		481.6956	625.3909

Table 4: Coag-flocculation kinetic parameters and linear regression coefficient of ALUM in PIE at varying pH and $0.3 \times 10^{-3} kg/m^3$ dosage.

Parameters	pH = 1	pH = 3	pH = 5	pH = 7	pH = 10	pH = 13
α	2.000	2.000	2.000	2.000	2.000	2.000
R^2	0.770	0.907	0.644	0.739	0.631	0.891
$K(m^3/kg.S)$	4.333E-06	1.139E-05	4.547E-06	5.296E-06	8.078E-06	1. 391E-05
$K_R(m^3/S)$	1.5392E-19	1.5463E-19	1.5877E-19	1.5571E-19	1.5668E-19	1.5699E-19
$\beta_{BR}(m^3/kg.S)$	8.666E-06	2.278E-05	9.094E-06	1.0592E-05	1.6156E-05	2.782E-05
$\varepsilon_p (kg^{-1})$	5.6302 E+13	1. 47323E+14	5.7278E+13	6.8024E+13	1.0311E+14	1.7721E+14
$\tau_{1/2}(Sec)$	501.71	127.24	318.73	182.64	134.65	312.57
(-r)	$4.333E-06C_t$	$1.139E-05C_t^2$	$4.547E-06C_t^2$	$5.296E-06C_t^2$	$8.078E-06C_t^2$	$1.391E-05C_t^2$
$C_o(kg/m^3)$	766.0487	931.6192	530.3633	1070.7785	867.9802	668.3152

Table 5: Coag-flocculation kinetic parameters and linear regression coefficient of ALUM in PIE at varying pH and $0.4 \times 10^{-3} kg/m^3$ dosage.

Parameters	pH = 1	pH = 3	pH = 5	pH = 7	pH = 10	pH = 13
α	2.000	2.000	2.000	2.000	2.000	2.000
R^2	0.666	0.939	0.421	0.687	0.432	0.714
$K(m^3/kg.S)$	3.409E-06	1.034E-05	8.391E-06	7.862E-06	3.998E-06	7. 255E-05
$K_R(m^3/S)$	1.5392E-19	1.5463E-19	1.5877E-19	1.5596E-19	1.5668E-19	1.5699E-19
$\beta_{BR}(m^3/kg.S)$	6.818E-06	2.068E-05	1.6782E-06	1.5724E-05	7.996E-06	1.451E-05
$\varepsilon_p (kg^{-1})$	4.4092 E+13	1. 3374E+14	1.0570E+14	1.05724E+14	5.1034E+13	9.2426E+13
$\tau_{1/2}(Sec)$	637.70	140.16	172.72	122.89	271.88	599.29
(-r)	$3.409E-06C_t^2$	$1.034E-05C_t^2$	$8.391E-06C_t^2$	$7.862E-06C_t^2$	$3.998E-06C_t^2$	$7.255E-06C_t^2$
$C_o(kg/m^3)$	645.7862	843.5259	490.9421	990.8839	1069.1757	505.076

Table 6: Coag-flocculation kinetic parameters and linear regression coefficient of ALUM in PIE at varying pH and $0.5 \times 10^{-3} kg/m^3$ dosage.

Parameters	pH = 1	pH = 3	pH = 5	pH = 7	pH = 10	pH = 13
α	2.000	2.000 2.000		2.000	2.000	2.000
R^2	0.680	0.938 0.669		0.657	0.449	0.77
$K(m^3/kg.S)$	4.43E-06	9.57E-06	4.06E-05	3.30E-06	5.95E-06	1. 06E-05
$K_R(m^3/S)$	1.5417E-19	1.5463E-19	1.5877E-19	1.5596E-19	1.5668E-19	1.5699E-19
$\beta_{BR}(m^3/kg.S)$	8.86E-06	1.914E-05	8.12E-05	6.60E-06	1.19E-05	2.12E-05
$\varepsilon_p (kg^{-1})$	5.7469 E+13	1. 2378E+14	5.1143E+14	4.2319E+13	7.5951E+13	1.3504E+14
$\tau_{1/2}(Sec)$	490.73	151.44	35.70	292.78	182.68	410.17

| (-r) | $4.43\text{E-}06C_t^2$ | $9.57\text{E-}06C_t^2$ | $4.061\text{E-}05C_t^2$ | $3.30\text{E-}06C_t^2$ | $5.95\text{E-}06C_t^2$ | $1.06\text{E-}05C_t^2$ |
| $C_o(kg/m^3)$ | 733.2991 | 815.0624 | 791.7030 | 1251.8778 | 1061.3458 | 570.1904 |

Table 7: Coag-flocculation kinetic parameters and linear regression coefficient of ALUM in PIE at varying pH and $0.6 \times 10^{-3}kg/m^3$ dosage.

Parameters	pH = 1	pH = 3	pH = 5	pH = 7	pH = 10	pH = 13
α	2.000	2.000 2.000	2.000	2.000	2.000	
R^2	0.937	0.870 0.936	0.499	0.607	0.654	
$K(m^3/kg.S)$	3.119E-06	9.864E-06	5.189E-05	1.495E-06	6.243E-06	1. 108E-05
$K_R(m^3/S)$	1.5443E-19	1.5463E-19	1.5877E-19	1.5596E-19	1.5699E-19	1.5724E-19
$\beta_{BR}(m^3/kg.S)$	6.238E-06	1.9728E-05	1.0378E-04	2.99E-06	1.2486E-05	2.216E-05
$\varepsilon_p\ (kg^{-1})$	4.039E+13	1. 2622E+14	6.536E+14	1.9172E+13	7.9533E+13	1.4093E+14
$\tau_{1/2}(Sec)$	696.99	146.93	27.93	646.28	174.11	392.40
(-r)	$3.119\text{E-}06C_t^2$	$9.864\text{E-}06C_t^2$	$5.189\text{E-}05C_t^2$	$1.495\text{E-}06C_t^2$	$6.243\text{E-}06C_t^2$	$1.108\text{E-}05C_t^2$
$C_o(kg/m^3)$	764.43675	884.4861	969.0862	1627.0745	750.2438	683.0601

Table 8: Coag-flocculation kinetic parameters and linear regression coefficient of ALUM in PIE at varying pH and $0.7 \times 10^{-3}kg/m^3$ dosage.

| Parameters	pH = 1	pH = 3	pH = 5	pH = 7	pH = 10	pH = 13
α	2.000	2.000 2.000	2.000	2.000	2.000	
R^2	0.916	0.849 0.985	0.765	0.675	0.842	
$K(m^3/kg.S)$	9.95E-06	1.14E-05	3.87E-05	4.423E-06	6.20E-06	6.29E-06
$K_R(m^3/S)$	1.5468E-19	1.5468E-19	1.5877E-19	1.5622E-19	1.5699E-19	1.5724E-19
$\beta_{BR}(m^3/kg.S)$	1.99E-05	2.28E-05	7.74E-05	8.46E-06	1.24E-05	1.56E-05
$\varepsilon_p\ (kg^{-1})$	1.0447E+14	1. 4740E+14	4.8750E+14	5.4154E+13	7.8986E+13	8.0005E+13
$\tau_{1/2}(Sec)$	218.48	127.13	37.45	228.41	175.32	691.23
(-r)	$9.95\text{E-}06C_t^2$	$1.14\text{E-}05C_t^2$	$3.87\text{E-}05C_t^2$	$4.23\text{E-}06C_t^2$	$6.20\text{E-}06C_t^2$	$6.29\text{E-}06C_t^2$
$C_o(kg/m^3)$	689.1799	689.1799	897.6661	1680.6723	1416.4306	676.1325
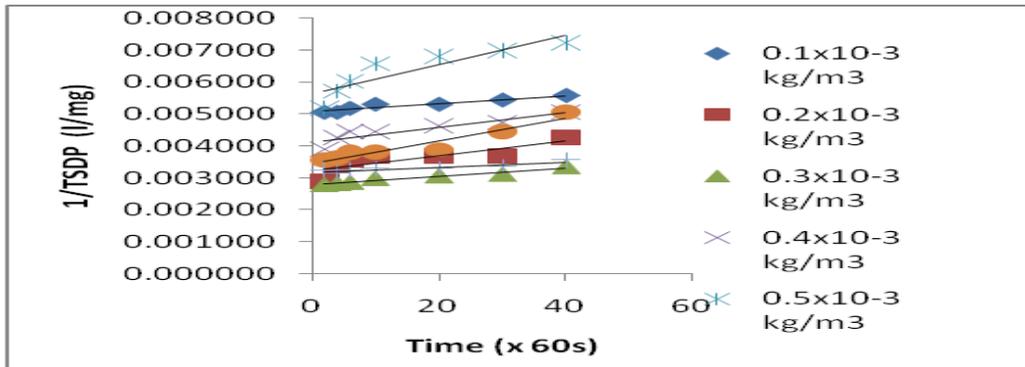
Fig 1: Selected Linear Plot Of 1/TSDP Vs Time For Ph=1
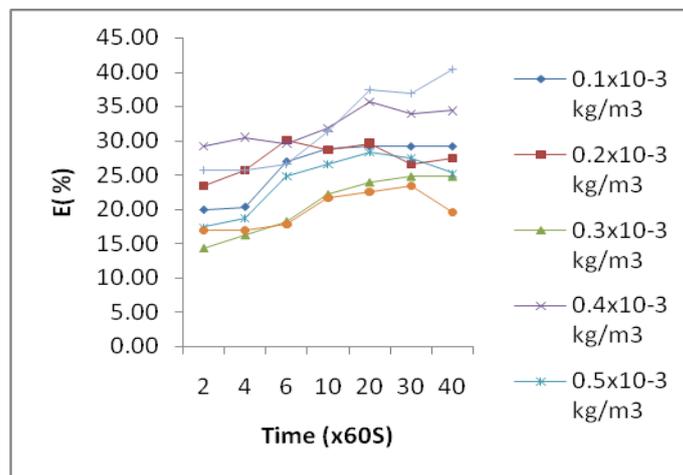

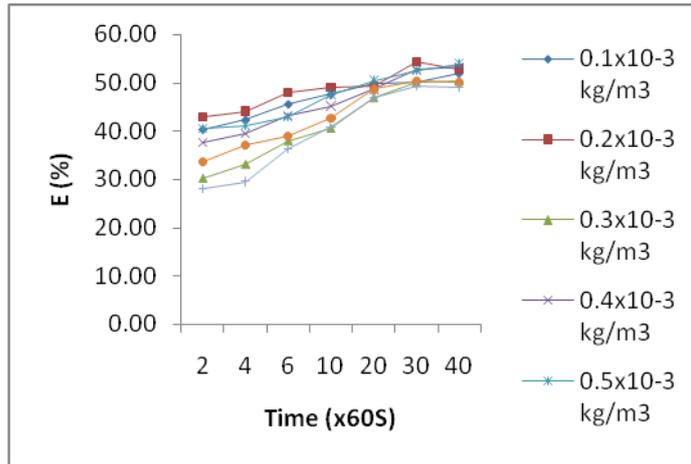**Fig 2: Selected Plot of E (%) Vs Time For Ph=1**

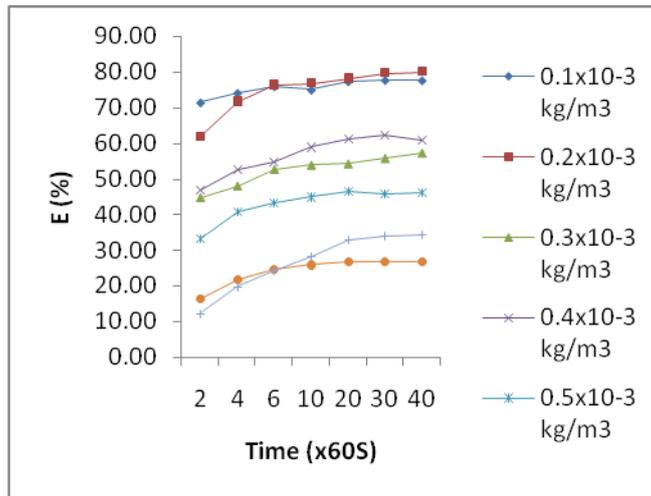**Fig 3: Selected Plot of E (%) Vs Time For Ph =3**

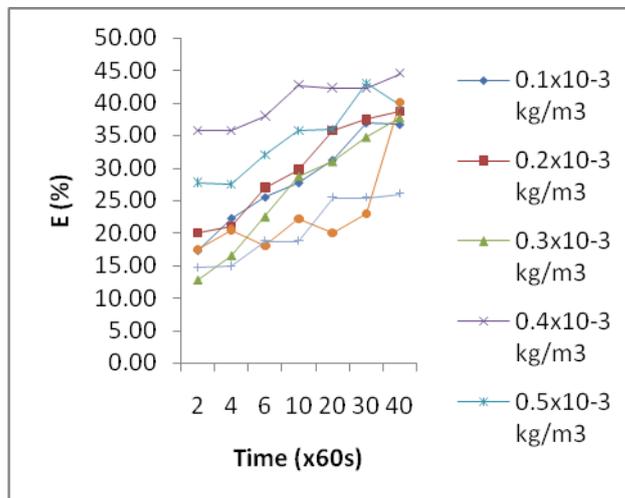**Fig 4: Selected Plot of E (%) Vs Time For Ph=7**

Fig 5: Selected Plot of E (%) Vs Time For Ph=13
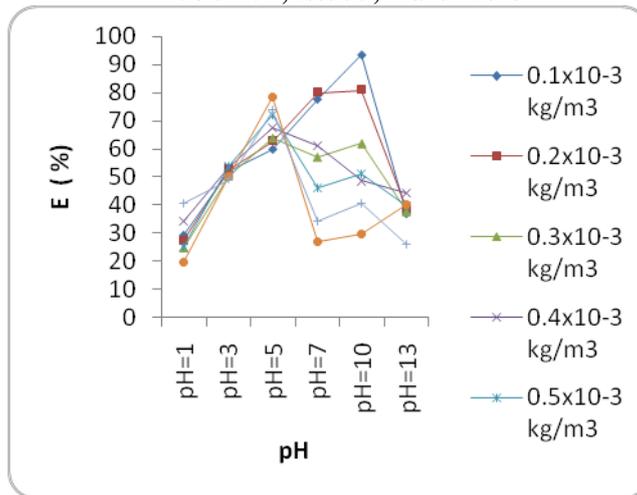
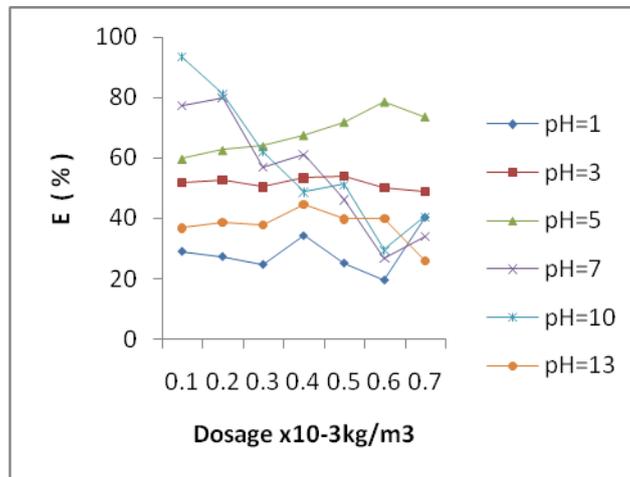**Fig 6: Plot of E (%) Vs Ph at 2400secs. For Varying Alum Dosage**

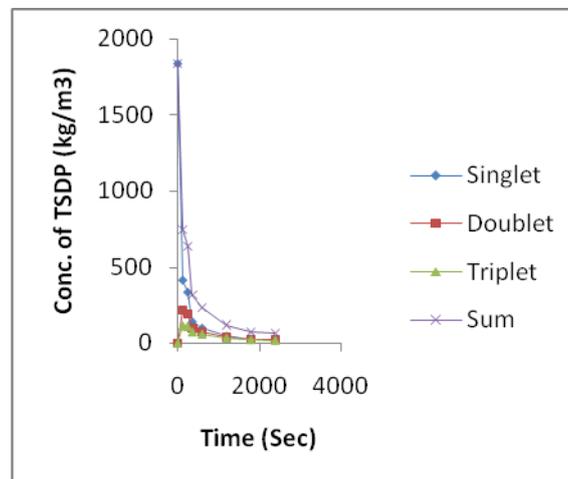**Fig 7: Plot Of (E %) VS Dosage (ALUM) At 2400secs. For Varying Ph**

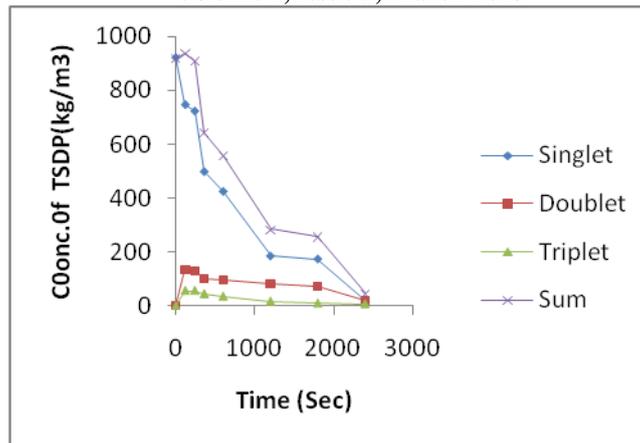**Fig 8: Particle Distribution Plot (Alum) For Minimum Half Life of 8.11sec**

Fig 9: Particle distribution plot (ALUM) for maximum half life of 929.50Sec

IV. RESULTS AND DISCUSSION

Plot of Efficiency E (%) Vs Time

These are presented in figs. 2 to 5. The significant feature of the figures show that turbidity (TSDP) removal efficiency increases with – increasing time for all pH and dosages. At 40 mins of time maximum removal of 93.26% is recorded at pH of 10 (0.1 x 10^{-3}kg/m^3). Though the value recorded at pH of 7 (0.1 x 0.2) x 10^{-3} kg/m^3 are impressive. It is observed that starting from t = 4 mins, there is minimal variation in E (%) values by a factor of ± 3 for pH of 10 (0.1 x 10^{-3}). The physical implication is that at least 86.09% and 93.26% of the initial TSDP load of 2560mg/l were removed at 4 mins and 40mins respectively. With the least E > 85%, it confirms the effectiveness of alum to remove turbidity (TSDP) from PIE at the least dosage in alkaline region. This phenomenon supports the theory of fast coagulation which is obtainable in real life coag-flocculation proceses.

Plot of Efficiency E (%) Vs pH

This is represented in fig 6. It indicates the performance of various doses of alum at varying pH. Coag-flocculation performance of alum at pH of 7 is close to that of pH of 10 for all pH and dosages. It is observed from the fig. that the best performance of alum in removing turbidity (TSDP) from PIE is obtained at pH of 10 followed by pH of 7 for (0.1 and 0.2) x 10^{-3}kg/m^3 dosages respectively. However, the highest turbidity (TSDP) removal is attained at pH of 10 for 0.1 x 10^{-3}kg/m^3 dosage. This is an indication that alum dosage for good coag-flocculation performance is almost narrow in this study. The important feature in this fig., show that with increase in pH, the turbidity (TSDP) removal increased and is found to be maximum at pH of 10 for (0.1 and 0.2) x 10^{-3}kg/m^3 dosages. This occurrence could be attributed to the optimum hydrolysis of alum at the pH of 10 for (0.1 and 0.2) x 10^{-3}kg/m^3 dosages. The hydrolysis of these coagulants particles enhances the ionic strength of the medium hence improving its efficiency [25]. The removal efficiency is remarkable

reduced when pH is further raised beyond 10 for all dosages. This reduction is attributed to the high concentration of hydroxyl ion that will complete with TSDP for adsorption sites. In addition, settling of metal hydroxides is inevitable at high pH[10],[26]. The phenomenon justifies the convergence of the particle kernels at the pH of 13 for almost all the dosage.

Plot of Efficiency E (%) Vs Dosage.

This is presented is fig. 7. It confirms the observations made from figs. 2 to 6. Fig. 7 actually represents how changes in coagulant dosage affected coag-flocculation efficiency. The significant feature is that the turbidity (TSDP) removal efficiency as a result of variation in the coagulant dosage did not follow any particular trend. However, for the optimum dosage of 0.1 x 10^{-3}kg/m^3, the system recorded the highest turbidity removal efficiency of 93.26%. From the dosage of (0.1 to 0.2) x 10^{-3}kg/m^3, the turbidity (TSDP) removal efficiency decreased. This phenomenon could be explained based on charge density. Comparatively with other coagulants, aluminum sulphate (alum) has a high charge density [27]. The charge density increases when alum hydrolyses in water to form aluminum hydroxides which will eventually produce short polymer chain that enhances microfloc formation [25]. Thus increasing the TSDP adsorption on polymerized alum, having more available attachment sites. This signifies the rapid destabilization of the particles at low dosage. Similarly, increasing the dosage from (0.2 to 0.7) x 10^{-3}kg/m^3, there is drastic decrease in the TSDP removal efficiency. This poor performance could be attributed to the phenomenon of excess polymer being adsorbed on the colloidal surfaces and producing restabilized colloids. Thus, there were no sites available on the particle surfaces for the formation of inter particle bridges. In addition, it is understandable that alum is rapidly hydrolyzed in water to give a range of products including cationic complexes which can be adsorbed by negatively charged particles (TSDP) and neutralize their charge. This is one mechanism whereby particles can be destabilized, to encourage flocculation. Over dosing can disrupt this phenomenon. Therefore, relative precise

control of coagulant dosage should be considered in water treatment plants.

Coagulation – Flocculation And Regression Coefficient Parameters.

The regression coefficient (R^2) were evaluated from the linearized selected plot of equation (26) known as fig1. The values obtained are presented in tables 2 – 8. In general, the values R^2 presented are more in the vicinity near one for the pH 1, 3, 5 and 13. Though the maximum value of R^2 is recorded at the optimum pH = 5. This is an indication that the process of adhesion of TSDP on aluminum hydroxide flocs formed during alum hydrolysis is controlled by monolayer sorption mechanism. Also this high values of R^2, confirms the theory of micro kinetics that show $\alpha = 2$. Equation (7b), show that α affects K inversely which implies that low value of α is a condition for high value of K. For $K = 0.5\beta_{BR}$, designated as equation 8, there is no defined observed pattern, as the pH and dosages increases from 1 – 13; and $(0.1 – 0.7) \times 10^{-3}kg/m^3$ respectively, for tables 2 – 8. However, it should be observed that the highest value of K for the process is recorded at pH of 10 and $0.1 \times 10^{-3}kg/m^3$ dosage with corresponding low value of $\tau_{1/2}$, thus amplified the fact that the best performances at the conditions of these experiments were achieved at alkaline medium for all the dosages except $(0.4, 0.5$ and $0.7)$ $10^{-3}kg/m^3$ where optimum value is achieved at pH of 5 and $0.5 \times 10^{-3}kg/m^3$ dosage. This phenomenon is an indication that coagulation – flocculation is favored more for alum in alkaline medium following easy hydrolysable in the effluent to form cationic complexes for TSDP sorption sites[25]. Also, since K is the rate at which two or more potential coagulating particles approaches each other[23]. It is understandable that K is associated with energy barrier between these intending coagulating particles caused by the presence of repulsive forces between them. At high K, the energy barrier between these possible coagulating particles is reduced at lowest $\tau_{1/2}$ following fast coagulation – flocculation process. The variation in K_R is generally minimal as presented in tables 2 – 8. This is becos K_R is dependent on temperature (T) and Viscosity (η) of the effluent medium and both of which did not vary substantially during the study. At vicinity near to a unit of K_R values, ε_p relates to $2K = \beta_{BR}$ directly (i.e $2\varepsilon_p = 2K = \beta_{BR}$) based on the evaluation of combined equations of (8) ,(9). The implication is that high ε_p results in high kinetic energy to overcome the potential energy barrier. This will result in colloidal destabilization to actualize low $\tau_{1/2}$ in favour of K (fast rate of aggregation). Also from equation (32), it can be deduced $\tau_{1/2}$ is a function of K and C_o, (initial TSDP concentration) mathematically expressed as $\tau_{1/2} = fn (C_o, K)^{-1}$. The implication of equation (32) is that the higher the C_o, the lesser the $\tau_{1/2}$. This is in support of high rate of settling obtainable in high turbidity waters. From equation (7a), rate equation (-r) $(-dC_t/dt)$ relates directly with K and C_t. The implication is that high rate constant

K results in high (-r) as can be observed in tables 2 – 8. The deviation of some functional parameters (K, K_R, ε_p, $\tau_{1/2}$) values from the general norms could be attributed to non-homogeneity of TSDP and Alum in PIE throughout the dispersion before flocculation sets in. This phenomenon could result in uneven distribution of TSDP/ Alum complexes in the mixing phase. This problem will make it impossible to achieve micro kinetics conditions where $\alpha = 2$[28]. Also this could lead to TSDP acquiring surface charges due to unequal distribution of constituent ions on the particle surface, giving way to preferential adsorption of specific ions, ionization of surface groups, crystal imperfection, or any combination of these. Another account is the effect of interchange of action and reaction between and among the attractive forces, repulsive force, and hydrodynamic interactions (arising from mechanical agitation) which invariably increases or reduces the values of parameters presented in tables 2 – 8.

V. PARTICLE DISTRIBUTION PLOTS

These are presented in figs 8 and 9 for $\tau_{1/2} = 8.11$ sec and $\tau_{1/2} = 929.50$ sec. In figure 8, for the curves of sum and singlets, they passes through a maximum (at N = 1840) because they are absent at t = 0, and at the end of coagulation/ flocculation process (40 mins) t = ∞, $\Sigma N_i = 69$ and $N_1 = 26$. The number of singlets can be seen to decrease more rapidly than the sum of the particles. This depicts a moderately hyper slope at early stage (120 sec) of coagulation/ flocculation process. Whereas the curves of doublets and triplets passes through the origin of t = 0, N = 0. At 600 sec. the singlets, doublets and triplets are close such that their variation with time are near same to t = ∞ . The curves at t = 600 sec show that there is a narrow margin difference in concentration of TSDP between the singlets, doublets, triplets and sum of particles. The curves are expected in coagulation-flocculation where there is existence of minimal colloidal entrapment and low shear resistance. The implication is the existence of small shear force resulting to resistance to collision. This is clearly demonstrated by the value of $\tau_{1/2}$, which runs into units of seconds instead of sub seconds as obtained by[20]. This is an indication of low zeta potential associated with the process. Conversely, in fig 9, the sum of particles and singlets decreases linearly with time under the influence of moderate shear force between them. Also for the doublets and triplets there is presence of shear resistance between them. The implication is the existence of potential hump created between them by a way of double layer formation. Furthermore, there is wide gap between the pairs of (sum of particles and singlets) and (doublets and triplets), which narrows down as the coagulation/flocculation process progresses until it gets to optimum period. This phenomena show a process being dominated by high repulsive forces, prohibiting the particles to come closer. The unique nature of the formation of singlets, doublets

and triplets in fig 8, indicates presence of moderate energy barrier.

VI. CONCLUSION

The effectiveness of aluminum sulphate in the reduction of total suspended and dissolved particles inherent in pharmaceutical, industry effluent has been reassured.

NOMENCLATURE

K: αth order coag-flocculation constant

β_{BR}:   Collision factor for Brownian transport

ε_p: Collision Efficiency

$\tau_{1/2}$:   Coagulation period/ half life.

R^2:   Regression coefficient of Determination

α: Coag-flocculation reaction order

E: Coag-flocculation Efficiency

K_R: Smoluchowski coag-flocculation constant.

-r: Coag-flocculation reaction rate

PIE: Pharmaceutical industry effluent

Alum: Aluminum sulphate

REFERENCES

[1] Overcash, M/R (1986). Techniques for industrial pollution prevention. A compendium for hazardous and non-hazardous waste minimization, lewis publishers, Inc. Michigan.

[2] Hashmi, I. (2005). Wastewater monitoring of pharmaceutical industry: Treatment and Reuse options. Electronic Journal of Environmental, Agricultural and food chemistry. 994 – 1004.

[3] Garcia, A. Rivas, H.M, Figueroa, J.L, Monroe, A.L (1995). Case history: Pharmaceutical wastewater treatment plant upgrade, smith kline Beecham Pharmaceuticals company. Designation. 102 (1-3): 255 -263.

[4] Chellapan, S. Sallis P. j. (2011). Application of anaerobic biotechnology for pharmaceutical wastewater treatment. The IIOAB journal. Special issue on environmental management for sustainable development 2 (1):13 – 21.

[5] Fox, P., Venkatasubbiah, V. (1996). "Coupled anaerobic/ aerobic treatment of high-sulpate wastewater with sulfate reduction and biological sulfide oxidation. "water SC. Techol., 34, 359 – 366.

[6] Muhammad, S. (2007). Pharmaceutical wastewater treatment. A physicochemical study. Journal of research (science), Bahauddin Zakariya university, Multan, Pakistan, 18 (2): 125 – 134.

[7] Ugonabo, V.I, Menkiti, M.C, Onukwuli, O.D. Effect of coag-flocculation kinetics on telfairia occidental's seed coagulant (TOC) in pharmaceutical wastewater. Proceedings of the 2012 national conference on infrastructural development and maintenance in the Nigerian Environment, Nnamdi Azikiwe university, Awka, Nigeria, 2012 179 – 190.

[8] Mayabhate, S.P, Gupta, S.K, Joshi, S.U (1988). Biological treatment of pharmaceutical wastewater. Water Air soil. Poll 38:189 – 197.

[9] Ugonabo, V.I, Menkiti, M.C, Onukwuli, O.D. (2012. Effect of Mucuna seed coagulant on total dissolved solid particles removal efficiency in pharmaceutical effluent medium by coag-flocculation process. Now York science journal 5(9): 75-85)

[10] Stephenson, R.J., Duff, S.J.B (1996). Coagulation and precipitation of a mechanical pulping effluent: Removal of carbon, colour and turbidity, wat. Res. 30 (4): 781 – 792

[11] Bina, B., Mehdinejad, M.H, Nkaeen, M. Movahedian, A.H (2009). Effeteness of chitosan as natural coagulant aid in treating turbid Waters Iran J. Environ. Health Sci. Eng. 6 (4) 247 – 252.

[12] McCarthy, J.F., Zachara, J.M (1989). Subsurface transport of Contaminants Environ. Sci. Techol 23 (5): 496 – 502.

[13] Exall, K.N, Vanloon, G.W; (2003). Effects of raw water conditions on solute state aluminum speciation during coagulant dilution. Water Res; 37:3341 – 3350

[14] Akitt, J.W, Farthing, A. (1981). Aluminum – 27 nucleat magnetic resonance studies of the hydrolysis of aluminum (iii). Part 5 slow hydrolysis using aluminum metal, J. chem.. Soc Dalton Trans. 1624 – 1628.

[15] Parker, D.R., Bertsch, P.M (1992). Identification and qualification of the Al13 tridecameric polycation using Ferron, Environ. Sci. technol. 26, 908 – 914.

[16] Thomas, F. Masion, A., Bottero, J.Y, Rouiller, J., Montigny, F. Genevrier, F. (1993). Aluminum (iii) Speciation with hydroxyl carboxylic-acids-Al-27 NMR study Environ. Sci. Technol. 27, 2511 – 2516.

[17] Duan, J. Gregory, J. (2003). Coagulation by hydrolyzing metal salts. Adv. Colloid interface sci., 100 – 102, 475 – 502.

[18] Ebeling, J.M, Sibrell, P.L, Ogden, S.R., summer felt, S.T (2003). Evaluation of chemical coagulation – flocculation aids for the removal of suspended solids and phosphorus from intensive recirculating aguaculture effluent discharge. Aquacultural Engineering 29, 23 – 42.

[19] Abbot and Van Ness. Schaum's outline of Theory and problems of thermodynamics, McGraw – Hill, New York, 1972.

[20] Hunter, R.J Introduction to modern Colloid science. (4th ed.). New York: University press. 1993.

[21] Menkiti, M.C. and Onukwuli, O.D. Coag-flocculation studies of Moringa Oleifera coagulant (MOC) in brewery effluent: Nephelometric approach. Journal of American Science, 2010, 6 (12), 788 – 806.

[22] Von Smoluchowski, M. "Versucheiner Mathematischem theories der koagulations kinetic kolloider lousungen. "Z. phys. Chem.. 1917, 92, 129 – 168.

[23] Fridrikhsberg, D.A. A course in colloid chemistry, M. publishers Moscow, Russia, 1984, 266 – 268

[24] AWWA, 2005. American water works association, standard methods for the examination of water and wastewater effluent, New York, USA.

[25] Baisali-sarkar, P.P, Chakrbarti, A. Vijay Kumar, V.K. Wastewater treatment in dairy industries – possibility of reuse. Desalination. 2006, 195, 141 – 152.

[26] NIK, N.N.A, Ahmad, Z.A., Muhammad, H.I, Mohd, O. A.K Chemical Coagulation of settle able solid-free palm oil Mill effluent (POME) for organic Load Reduction. Journal of industrial Technology. 2001, 10 (1), 55 – 72.

[27] National Water qualify management strategy, Australian Drinking water guidelines, Drinking water treatment chemicals, draft for public consultation, and 2005.

[28] 28. Yates, P., Yan, Y. Jamson, G.J and Biggs, S. "Hetero aggregation of particle system: Aggregation mechanisms and aggregates structure determination"

[29] Melbourne, Australia, 23 – 27, 2001, 1 – 10.